Deamidation in Human γS-Crystallin from Cataractous Lenses Is Influenced by Surface Exposure†

Veniamin N. Lapko,‡ Andrew G. Purkiss,§ David L. Smith,‡ and Jean B. Smith*,‡

Department of Chemistry, University of Nebraska, Lincoln, Nebraska, and School of Crystallography, Birkbeck College, London, United Kingdom

Received November 9, 2001; Revised Manuscript Received May 1, 2002

ABSTRACT: A major component of human nuclear cataracts is water-insoluble, high molecular weight protein. A significant component of this protein is disulfide bonded γS-crystallin that can be reduced to monomers by dithiothreitol. Analysis of this reduced γS-crystallin showed that deamidation of glutamine and asparagine residues is a principal modification. Deamidation is one of the modifications of lens crystallins associated with aging and cataractogenesis. One proposed hypothesis of cataractogenesis is that it develops in response to altered surface charges that cause conformational changes, which, in turn, permit formation of disulfide bonds and crystallin insolubility. This report, showing deamidation among the disulfide bonded γS-crystallins from cataractous lenses, supports this hypothesis.

In this study, deamidation was quantified at all glutamine and asparagine residues of γS-crystallins isolated from human nuclear cataracts, both from the soluble portion and from high molecular weight proteins of the insoluble portion. Comparison of deamidations in soluble and insoluble γS-crystallins suggests that deamidation at some sites is associated with protein insolubility. Because the extent of deamidation was determined for all glutamines and asparagines in γS-crystallin, the relationship between the extent of deamidation and the surface accessibility of each residue could be evaluated. Accessibilities were calculated either from the recently published crystal structure of the C-terminal region of human γS-crystallin or from homologous residues in the N-terminal region of bovine γB-crystallin. This relationship showed residues with low accessibility have minimal deamidation while those with higher accessibility have a range of deamidation, indicating that accessibility of glutamines and asparagines is a major factor in their deamidation.

The proteins of the human eye lens, called crystallins, accumulate throughout life with the oldest proteins in the nucleus and the more recently synthesized in the cortex. Because the lens crystallins do not turnover appreciably, there is ample opportunity for them to become modified as the lens ages. Results from numerous studies indicate that accumulation of these modifications leads to insolubility of a portion of the crystallins and eventually to opacity (*1*−*5*). A likely contributor to crystallin insolubility is deamidation at glutamine and asparagine residues. Deamidation increases with the age of the lens (*6*−*10*) and is more prevalent among the insoluble crystallins (*11*, *12*). Deamidation is also associated with cataract (*13*−*15*). A proposed hypothesis explaining the relationship between deamidation and crystallin insolubility is that conversion of a neutral amide to a charged unprotonated acid causes protein unfolding and instability, perhaps allowing disulfide bonds to form (*16*). The prevalence of disulfide bonds among insoluble crystallins is well established (*11*, *12*, *17*).

Testing this hypothesis has been a challenge because the water-insoluble proteins are a complex mixture, and it has been difficult to obtain the components sufficiently isolated for their identification. The water-insoluble proteins from cataractous lenses include a wide range of molecular masses (*18*, *19*) with contributions from both disulfide (*17*, *20*) and nondisulfide (*3*, *21*, *22*) cross-linked species. Recent studies in our laboratory have shown that the predominant disulfide cross-linked species in the water-insoluble portion of nuclear cataracts is γS-crystallin (Lapko, in preparation). Using several steps of chromatography, these nuclear γS-crystallins, which were intermolecularly disulfide bonded, were obtained in sufficiently pure form for quantitative analysis of deamidation. The extent of deamidation in insoluble γS-crystallins was compared with deamidation in water-soluble γS-crystallins from the same nuclear cataracts. At several residues, the insoluble γS-crystallins were more extensively deamidated than the soluble γS-crystallins. Comparison of the extent of deamidation at each residue of γS-crystallin with its position in the crystal structure (*23*) shows that the deamidation is strongly influenced by the surface exposure.

MATERIALS AND METHODS

Isolation of γS-Crystallin from the Water-Insoluble Portion of Nuclear Cataracts. This study included three lenses, ages 75, 76, and 87, classified as having age-related nuclear cataract. After removal by interocular surgery, each lens was immediately placed in 5−7 mL of a saline solution and

† This research was supported by a grant (EY RO1 07609) from the National Institutes of Health and the Nebraska Center for Mass Spectrometry.

* Address correspondence to Jean B. Smith, Department of Chemistry, Hamilton Hall, University of Nebraska, Lincoln, NE 68588-0304.

‡ University of Nebraska.

§ Birkbeck College.

10.1021/bi015924t CCC: $22.00
Published on Web 06/06/2002

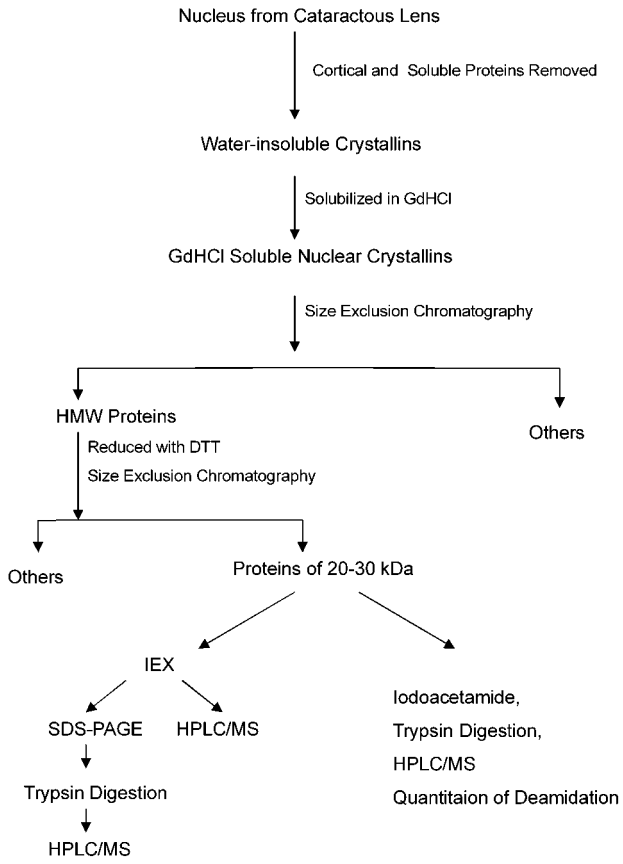

FIGURE 1: Isolation procedure for obtaining γS-crystallins from the high molecular weight protein of nuclear cataracts. The proteins of interest in this study were those that were reduced to 20−30 kDa by dithiothreitol.

transported to the lab on ice within 2 h. Visual inspection verified that the lenses were opaque. The 75-year-old lens was light brown; the 87- and 76-year-old lenses were yellow.

Each lens was processed and analyzed separately. The procedure for isolating the proteins is illustrated in Figure 1. Following removal of the saline solution, the remaining cortical proteins were solubilized by occasional swirling of the lens in a buffer of 50 mM MES,[1] 0.5 M NaCl, 1 mM EDTA, pH 6.2, containing protease inhibitors (Complete Mini protease inhibitor cocktail tablet, Boehringer, Mannheim, Germany) for 14−18 h at 0 °C. This pH was chosen to minimize thiol exchange and disulfide bond formation during isolation. After removal of the cortical proteins, the nuclear portion was transferred to 4 mL of the same buffer, homogenized by strong stirring, under argon, at 0 °C for 4 h. The homogenate was then centrifuged for 30 min at 33000*g*. The supernatant, which contained the soluble nuclear proteins, was removed. The pellet was again homogenized with 6 mL of MES buffer using a tissue grinder, centrifuged at 33000*g* for 15 min, and the supernatant solution was removed. To be certain that all water-soluble proteins were removed, the homogenization, centrifugation, and removal of supernatant steps were repeated three times.

[1] Abbreviations: MES, 2-(*N*-morpholino)ethanesulfonic acid; GdHCl, guanidine hydrochloride; EDTA, ethylenediamine tetracetic acid; DTT, dithiothreitol; HPLC, high-pressure liquid chromatography; MS/MS, tandem mass spectrometry; SDS−PAGE, sodium dodecyl sulfate−polyacrylamide gel electrophoresis; HMW, high molecular weight; SIM, selected ion monitoring.

The pellet remaining after removal of the water-soluble crystallins was again homogenized in 3 mL of the MES buffer containing 6 M guanidine hydrochloride (GdHCl). The pellets were completely solubilized after 16−24 h. The fact that the protein could be completely solubilized in GdHCl and the lenses were only light to medium yellow, indicated that these nuclear cataracts were type I or II (*24*). The homogenates were transferred to 1.5-mL microcentrifuge tubes and centrifuged for 25 min at 14 000 rpm. These GdHCl-soluble proteins were then separated chromatographically.

The GdHCl-soluble proteins from each lens nucleus (200 μL/analysis) were fractionated by size exclusion chromatography (Superose 12 HR 10/30 column, Pharmacia Biotech) with an elution buffer of 50 mM MES buffer, 6 M GdHCl, 1 mM EDTA, pH 6.2 at a flow rate of 0.25 mL/min. The eluted proteins were detected at 280 nm. The crystallins with molecular masses greater than 130 kDa (the HMW proteins) were reduced with 500 mM DTT at 37 °C for 24 h, and again separated by size exclusion chromatography under identical conditions with 10 mM DTT in the MES buffer. The HMW proteins that were reduced to molecular masses of 20−30 kDa by DTT, the crystallins of interest in this study, will be referred to as reduced HMW proteins. They were divided into two portions. The proteins in one portion were analyzed as intact proteins after ion exchange chromatography. These fractions were analyzed by reversed phase HPLC/MS and SDS−PAGE. The proteins in the other portion, without further separation, were digested with trypsin and analyzed as peptides to determine the extent of deamidation at each site.

Purification of Soluble γS-Crystallins. Soluble proteins from the nuclear cataracts were isolated by size exclusion separation (2.5 × 95 cm Toyo-Pearl HW-55sf column) with subsequent isolation of the γS-crystallins by reversed phase HPLC (0.46 × 15 cm Vydac column) as described previously (*8*).

Ion-Exchange Chromatography. Before fractionation by ion exchange chromatography, the reduced HMW proteins were desalted using a C-4 reversed phase column with a protein Macrotrap (Microchrom BioResources) and dried by vacuum concentration. For the anion exchange fractionation, the proteins were dissolved in 800 μL of a buffer (20 mM Tris-HCl, 8 M urea, 5 mM DTT, pH 7.6) and applied to a Mini Q column (Pharmacia) equilibrated with the same buffer. The 8 M urea solutions used to prepare the buffers were deionized immediately before use. The proteins were eluted at a flow rate 0.4 mL/min by a gradient of 0−80 mM NaCl developed over 32 min, followed by 80−110 mM NaCl in 10 min, and finally to 400 mM NaCl in 8 min. Collected fractions were placed on dry ice and stored at −80 °C.

SDS−PAGE Analysis of Ion Exchange Fractions. The ion exchange fractions were analyzed by SDS−PAGE (*25*). When the protein bands obtained from SDS−PAGE were to be digested in situ, they were visualized by negative Zn staining and processed according to a previously published protocol (*26*). The in situ digestion used sequencing grade modified trypsin (Promega) for 14 h at 37 °C at a protein/enzyme ratio of 30:1. Preparation of the digests of SDS−PAGE separated proteins for HPLC/MS analysis also followed a published protocol (*26*).

Online HPLC/Mass Spectrometric Analysis of Ion Exchange Fractions. The reduced HMW proteins separated by ion exchange were further analyzed by HPLC/MS. This apparatus consisted of an online capillary reversed phase HPLC (0.3 × 150 mm C4 column) connected directly to an electrospray ionization quadrupole time-of-flight mass spectrometer (QTOF, Micromass, Manchester, UK), with a flow rate of 5 μL/min, maintained by a microflow processor (AcuRate, LC-Packings). The HPLC used a gradient of 20−65% acetonitrile in water, both with 0.05% TFA, developed over 30 min. Uncertainty in the protein mass determinations was typically less than 0.005%. Protein elution was also monitored by UV absorbance at 280 nm.

Online HPLC/Mass Spectrometric Analysis of Tryptic Peptides. Peptides produced by tryptic digestion were analyzed by online reversed phase HPLC (0.3 × 250 mm, C18-PM, LC-Packings) connected directly to an electrospray ionization ion trap mass spectrometer (Finnigan MAT LCQ, San Jose, CA). The HPLC gradient was 0−50% acetonitrile in water, both with 0.01% TFA, over 50 min. The flow rate was 5 μL/min. Peptide elution was monitored at 214 nm. For tryptic mapping, the ion trap mass spectrometer was routinely operated in the full scan MS mode with the most abundant ion of each scan analyzed by MS/MS.

Determination of Extent of Deamidation. Tryptic peptides of reduced and iodoacetamide derivatized HMW proteins were used to determine the extent of deamidation at each glutamine and asparagine of γS-crystallin. Before digestion, the HMW proteins were desalted by a reversed phase protein trap and dried by vacuum concentration. The proteins were dissolved in a buffer (200 mM Tris-HCl, 1 mM EDTA, 0.5 mM DTT, pH 8.4) and treated with 15 mM iodoacetamide at room temperature in the dark for 20 min. The reaction was quenched by adding excess DTT. A similar procedure was used to prepare iodoacetamide derivatized γS-crystallins from the soluble proteins of nuclear cataracts. For trypsin digestion, an enzyme/protein ratio of 1:50 and a digestion time of 12 h were usually used. However, to obtain sufficient quantities of peptides 41−60 and 61−71, the proteins were digested starting with a trypsin/protein ratio of 1:40, the same amount of trypsin was added again after 3 h, and the digestion was continued overnight.

Different approaches were used to quantify deamidation at each site. With the reversed phase separation conditions used in this study, deamidated peptides eluted after their corresponding amidated species. The extent of deamidation in peptides 7−18 and 131−145, for which amidated and deamidated forms eluted as pure peptides, was determined from the relative UV absorbances (214 nm) of the peaks or from the MS responses. The extent of deamidation calculated from the UV and MS signals agreed within 10%.

The majority of tryptic peptides of interest coeluted with other peptides, sometimes as a minor component of a chromatographic peak. To quantify deamidations at Asn 53, Asn 76, and Gln 92, the total ion current in the zoom mode (default window ± 5 *m*/*z*) was used. If the selectivity of the zoom scan mode was not adequate, selective ion monitoring with a narrower *m*/*z* region was used. For peptides 7−18, 60−71, and 101−124, each of which contains two potential sites of deamidation, MS/MS analysis was used to identify the deamidated residues. In these experiments, a second deamidation could be detected if its contribution to the deamidation was 25−30%. Additional information was obtained from chymotryptic and Asp-N digests.

When only one peak was found for a peptide containing glutamines and/or asparagines, this peak was examined to determine whether it included both amidated and deamidated forms. The presence of deamidation could be detected from the isotopic pattern in the zoom scans. The extent of deamidation could be determined by comparing the experimental isotope pattern with the isotope pattern for this peptide without deamidation calculated from the natural abundance of C-13. This analysis used the Magtran program provided by Dr. Zhongqi Zhang (personal communication). Calculation of the extent of deamidation using isotope ratios has been described in detail in previous publications (*12*, *27*).

Calculation of Surface Exposure of Glutamines and Asparagines. The C-terminus of γS-crystallin contains six glutamines and one asparagine, while the N-terminus has four asparagines and three glutamines. To calculate the surface accessibilities of the glutamines and asparagines, a model of human γS-crystallin was made in which the C-terminal domain of human γS-crystallin (*23*) was superposed onto the C-terminal domain of complete bovine γB-crystallin (*28*) to obtain the orientation of the N-terminal domain relative to the C-terminal domain. Nonidentical residues in the N-terminal domain were then mutated to match the human γS-crystallin sequence. C-terminal accessibilities were calculated from the dimer found in the single domain crystal lattice (*23*), and N-terminal accessibilities were calculated from the model structure. All N-terminal asparagines and glutamines of γS-crystallin have homologous residues in bovine γB except Asn 14 and Gln 63, which are Gly 10 and Arg 59, respectively. The calculation used the program NACCESS (*29*) with a probe with a diameter of 1.4 Å (the same radius as water) rolled around the van der Waals surface of the macromolecule. The calculation makes successive thin slices through the 3D molecular volume to calculate the accessible surface of individual atoms.

RESULTS

The water-insoluble, GdHCl-soluble proteins of nuclear cataract are a complex mixture of proteins with a wide range of molecular masses. For the nuclear cataracts examined in this study, the high molecular weight (HMW) proteins, those with molecular weights greater than 130 kDa (Figure 2A), accounted for 17−33% of water-insoluble portion. After reduction of the disulfide bonds and rechromatography by size exclusion, 15−25% of these HMW proteins had molecular weights of 20−30 kDa, corresponding to monomers (Figure 2B). These proteins were chosen for detailed analysis in this study. On the basis of the molecular masses of peptides produced by tryptic digestion, γS-crystallin was identified as the major component of this fraction. Tryptic peptides from the entire backbone of γS-crystallin (Table 1) were found along with some minor peptides attributable to γC-, γD-, and βB1-crystallins. These results indicated that γS-crystallin is a major component of HMW aggregates formed by intermolecular S−S bonding.

Mass spectra of intact proteins in the 20−30 kDa fraction formed by DTT-reduction of HMW aggregates using online reversed phase HPLC/MS were not satisfactory. This was probably due to the presence of several modified forms of

Table 1: Tryptic Peptides of γS-Crystallin

peptide[e]	residues	sequence[d]	calculated mass[a]
T1	1−2	SK	275.1[c]
T2	3−6	TGTK	405.2
T3+4	7−18	ITFYEDKNFQGR	1516.7[b]
T5+6	19−35	RYDC*DC*DC*ADFHTYLSR	2252.7
T7	36−40	C*NSIK	620.3
T8	41−71	VEGGTWAVYERPNFAGYMYIL PQGEYPEYQR	3682.7
T9	72−78	WMGLNDR	890.4
T10	79−83	LSSC*R	621.3
T11	84−94	AVHLPSGGQYK	1155.6
T12	95−100	IQIFEK	776.4
T13	101−124	GDFSGQMYETTEDC*PSIMEQFHMR	2895.3
T14	125−130	EIHSGK	715.3
T15	131−145	VLEGVWIFYELPNYR	1897.0
T16	146−147	GR	231.1[c]
T17+18	148−154	QYLLDKK	906.5
T19	155−157	EYR	466.2
T20	158−173	KPIDWGAASPAVQSFR	1728.9
T21+22	174−177	RIVE	515.3

[a] The observed masses were with 0.2 Da of the calculated masses. [b] Masses were calculated for the amidated peptides. [c] Mass not observed. [d] Asterisk (*) corresponds to carboxyamidomethylcysteine. [e] Each peptide was identified by CID MS/MS.

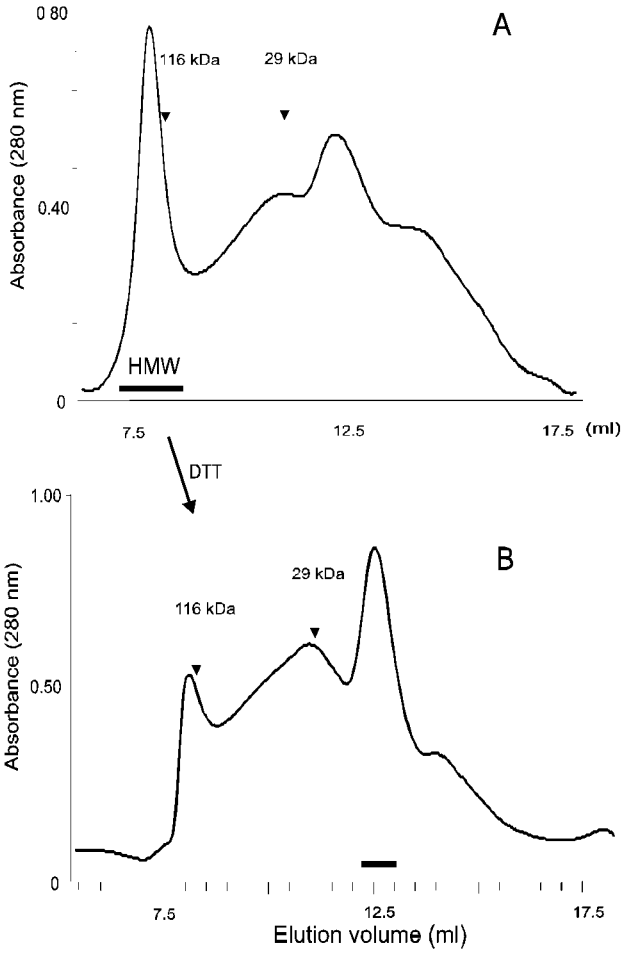

FIGURE 2: Size exclusion fractionation of (A) total insoluble proteins from a nuclear cataract. The HMW fraction is indicated by the bar. (B) the HMW fraction after reduction by DTT. The arrows indicate the elution volumes of carbonic anhydrase (29 kDa) and β-galactosidase (116 kDa). The fraction used in this study indicated by the bar.

γS-crystallin, some γC-, γD-, and βB1-crystallins in this fraction and the fact that HPLC did not give adequate separation of the proteins. Two separate approaches were used to examine these proteins. In the first approach, the intact proteins were fractionated by ion exchange and analyzed directly by HPLC/MS. The ion-exchange fractions were also analyzed by SDS−PAGE, followed by in-gel trypsin digestion and analysis of the peptides by HPLC/MS. These analyses served to identify the proteins in the ion-exchange fractions, but the quantity of peptides eluted from the gels was not sufficient to quantify deamidation. In the second approach, the total proteins from the 20−30 kDa fraction after DTT reduction were derivatized with iodoacetamide, digested with trypsin, and analyzed as peptides by HPLC/MS. The extent of deamidation at each glutamine and asparagine was determined from these analyses.

Characterization of Intact Proteins. To obtain samples of intact proteins amenable to MS analysis, the reduced HMW proteins were fractionated by anion-exchange chromatography. The chromatogram had four peaks (Figure 3). SDS−PAGE analysis of these anion exchange fractions (inset, Figure 3) showed that fractions 1, 3, and 4 had a major component of approximately 21 kDa. These data were supported by HPLC/MS analysis showing a molecular weight of 20 918 ± 1 Da as a principal component of these fractions. This mass corresponds to γS-crystallin (calculated M_r 20 918). Reconstructed mass spectra are shown for fraction 1 (Figure 4A) and fraction 3 (Figure 4B). In-gel digestion of the bands from ion exchange fraction 1 showed that, in addition to γS-crystallin, this fraction contained γC- and γD-crystallins (lower band, lane 1 of Figure 3) and truncated βB1-crystallin (the upper band). Reversed phase HPLC of the intact proteins of this fraction yielded a satisfactory mass spectrum only for γS-crystallin (Figure 4A). The proteins in fractions 5, 6, and 7 of the ion exchange separation did not produce useful MS spectra, probably because these fractions were extremely heterogeneous as indicated by the broad bands in the gel. In-gel digestion of the bands at 21 kDa from these fractions identified them as γS-crystallins.

Deamidation is the only modification known to decrease the charge of a protein with only a one mass increase per modification. Finding the same molecular mass γS-crystallin in all three ion exchange fractions indicated that deamidation was responsible for the decreased charge of the later eluting fractions. Even though mass spectra of the undigested γS-

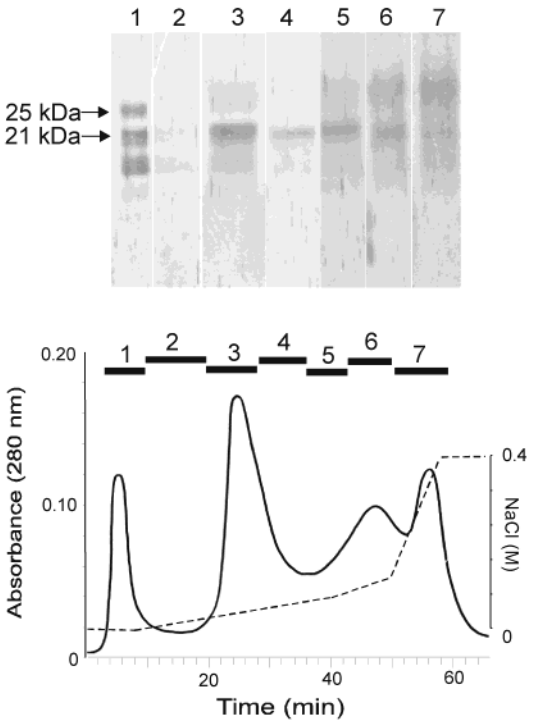

FIGURE 3: Anion exchange chromatogram of high molecular weight proteins that had molecular masses of 20−30 kDa after reduction by DTT. The analysis used a Mini Q column (Pharmacia) with an elution buffer of 20 mM Tris-HCl, 8 M urea, 1 mM DTT and a flow rate of 0.4 mL/min. The dashed line shows the gradient of NaCl (from 0 to 0.4 M). The combined fractions are shown by the bars. The inset at the top shows the SDS−PAGE analysis of the combined fractions. In this analysis, the approximate percent of the total proteins applied was 2% from fractions 1, 2, and 7, 1% from fractions 5 and 6, and 0.4% from fractions 3 and 4.

crystallins (Figure 4) showed a minor peak that may be an oxidized form (+16 Da) of the protein, no evidence of a peptide with an additional oxygen was seen in the tryptic digests. Failure to find oxidized peptides suggested that the oxidation was distributed among several sites, with not enough at any one site to be detected at the peptide level.

Location and Quantitation of the Deamidations of γS-Crystallin. The proteins isolated from the reduced HMW fraction contained primarily γS-crystallin with only minor contamination from other crystallins. With this level of purity, it was possible to quantify deamidation at each site of γS. Online HPLC/MS analysis of tryptic digests of the reduced HMW proteins provided a UV chromatogram of the separated peptides (Figure 5), the masses of the peptides (MS), and their collision induced fragments (CID MS/MS). Each peptide was identified by its mass and its MS/MS fragmentation pattern. The MS/MS spectra were also used to locate deamidated residues. With the HPLC conditions used in the present study, deamidated peptides eluted after the amidated forms, as indicated by the asterisks in Figure 5. The molecular masses of peptides in these peaks, one mass unit larger than expected (Table 1), showed that they were deamidated forms of γS-crystallin peptides.

The method used to determine the extent of deamidation depended on the composition of the peaks in which the deamidated and amidated peptides eluted. Mass spectra showed how many peptides were present in each peak and identified them. When the amidated or deamidated forms of the peptide eluted in separate peaks and no other peptides eluted with either, as was the case for peptides 7−18 and 131−145, the level of deamidation was calculated from the relative UV absorbances of the peaks for the pure peptides.

The use of MS spectra and UV absorbances for quantitating deamidation is illustrated for peptide 7−18 (T3 + T4). The amidated form of peptide 7−18 eluted at 38.8, while deamidated forms eluted at both 40.3 and 40.6 min (inset A, Figure 5). The MS/MS spectrum for the amidated peptide (38.8 min, Figure 6A) showed all the fragments of the y series with the expected masses calculated from the sequence given at the top of the Figure 6. The MS/MS spectra for the peptides eluting at 40.3 and 40.6 min both showed y_5-y_{10} one mass higher than the calculated values, indicating Asn 14 was deamidated, but Gln 16 was unmodified (Figure 6B). A very minor amount of another deamidated form of peptide 7−18 eluting at 41.3 min showed a two mass increase indicating deamidation at both Asn 14 and Gln 16. Modification at both amides was confirmed by MS/MS (Figure 6C). No peptide deamidated only at Gln 16 with intact Asn 14 was detected. MS/MS spectra of singly deamidated peptide 7−18 always showed deamidation only at Asn 14. These results suggest that deamidation at Asn 14 might be a precursor of deamidation at Gln 16. The extent of deamidation at Asn 14 (60 ± 10%) was calculated by comparison of the UV absorbance at 38.8 min (amidated) with the sum of the UV absorbances at 40.3 and 40.6 min (both with Asn 14 deamidated). The additional deamidation in the peptide eluting at 41.3 min contributed no more than 5%.

In peptide 131−145, there is only one possible site of deamidation, Asn 143. The 50% deamidation calculated by comparison of the absorbances at 63.0 min (amidated) and the sum of the absorbances at 63.7 and 64.1 min (both deamidated) (inset B, Figure 5) could be assumed to be at Asn 143. This assumption was confirmed by comparison of MS/MS spectra of the amidated and deamidated peptides (spectra not shown).

Observation of two HPLC peaks for deamidated peptide 7−18 (inset A, Figure 5) and deamidated peptide 131−145 (inset B, Figure 5) is likely due to isomerization of aspartic acid to form β-aspartic acid. Peptides which contain β-aspartic acid usually elute on reversed phase HPLC before α-aspartic acid forms. This observation has been confirmed in our laboratory where the α and β forms have been identified by their reactivity with the enzyme, Asp-N, which cleaves N-terminally to α-aspartic acid, but not to β-aspartic acid (V. Lapko, unpublished data). The aspartic acids at residues 11 and 14 in deamidated peptide 7−18 and at residue 143 in deamidated peptide 131−145 may undergo in vivo racemization/isomerization. This phenomenon, previously reported for Asp residues of α-crystallins (*30*, *31*), has also been observed in our laboratory (V. Lapko, unpublished data).

In cases where the peptides of interest coeluted with other tryptic peptides, deamidation was quantified using the zoom scan mode of the mass spectrometer. For example, tryptic peptide 41−71 (T8) coeluted with peptides from γC and βB1. This peptide contains three potential deamidation sites. To determine the number of deamidations in peptide 41−71, ions at *m*/*z* 1229.5 ± 5, the triply charged form of the peptide (MW 3685.1), were monitored in the zoom scan mode as the peak eluted (Figure 7A). Different regions of the peak are designated as a−d in the total ion current plot.

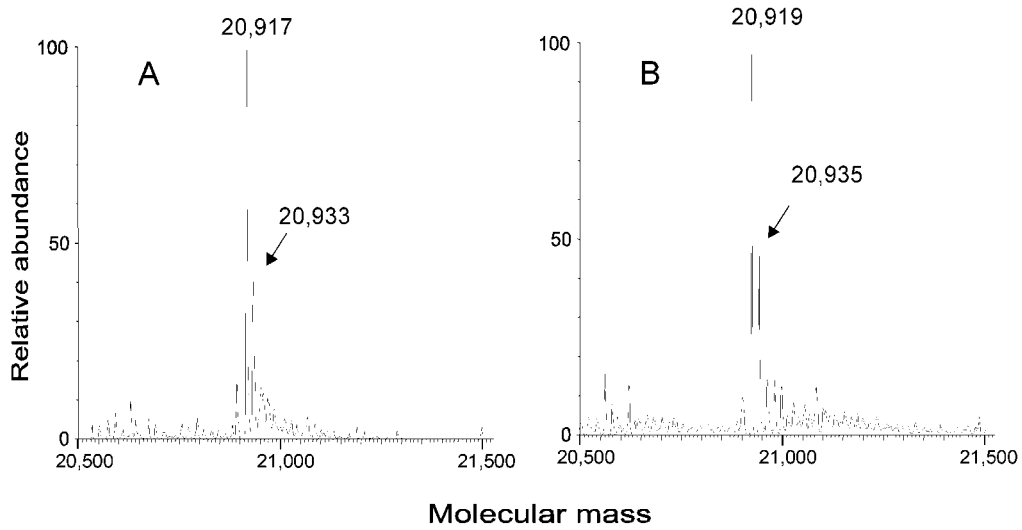

FIGURE 4: Reconstructed electrospray ionization mass spectrum of γS-crystallins after isolation by ion exchange (A) fraction 1 of Figure 3, and (B) fraction 3 of Figure 3.

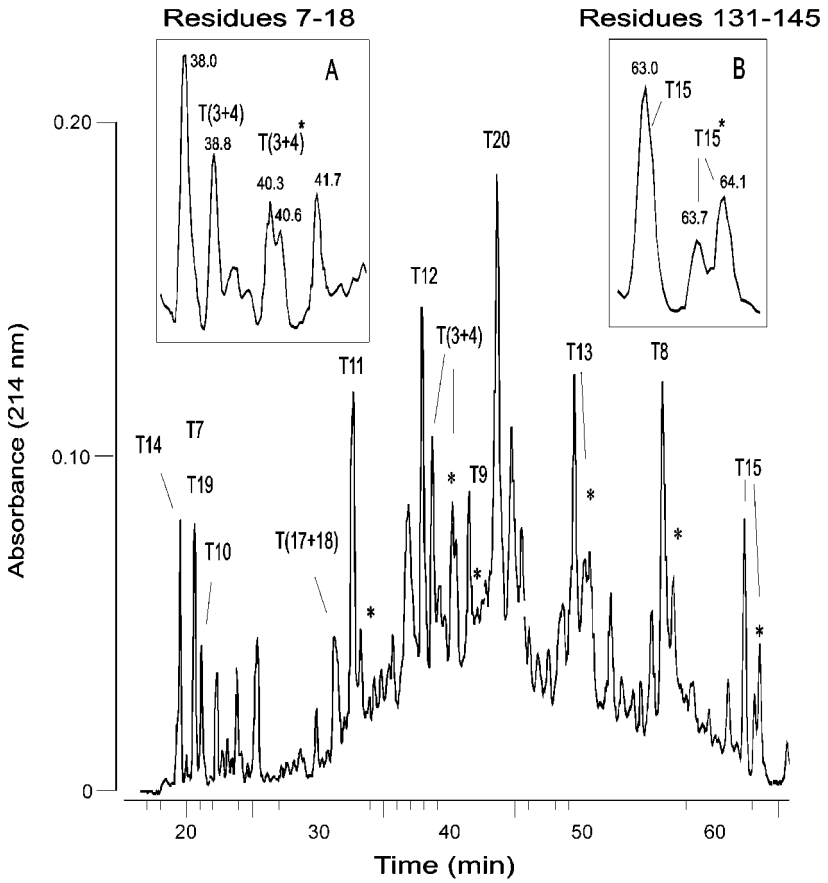

FIGURE 5: UV chromatogram of an online reversed phase HPLC/MS analysis of a tryptic digest of the high molecular weight proteins that had molecular masses of 20−30 kDa after reduction by DTT. Peaks containing tryptic peptides of γS-crystallin are indicated by "T" and correspond to the residues marked in Table 1. Major deamidated peptides are marked by an asterisk. The insets, A and B, show expanded regions from 37.5 to 42 min for peptide T(3+4) and from 62 to 65 min for peptide T15, respectively. Elution times of peptides are indicated on the top of the peaks.

The mass of the peptide eluting in each region is given in the figure. The major response in region "a" was due to the unmodified peptide (*m*/*z* 1229.3). Masses 0.4 Da higher (*m*/*z* 1229.7) for the triply charged ions, found in regions "b" and "c", correspond to a one mass unit increase in the peptide, indicating the peptides eluting in both "b" and "c" are singly deamidated. Region "d" contained the peptide with two deamidations (*m*/*z* 1230.0).

The approach for identifying deamidation at each site in a peptide with several possible deamidation sites is also illustrated by the MS/MS analysis of peptide 41−71, eluting in region "b". The sequence for peptide 41−71, which has potential deamidation sites at Asn 53, Gln 63, and Gln 70, and masses of several fragments in the y-series of the unmodified peptide are given at the top of Figure 7B. Information specific to Gln 70 can be obtained from the

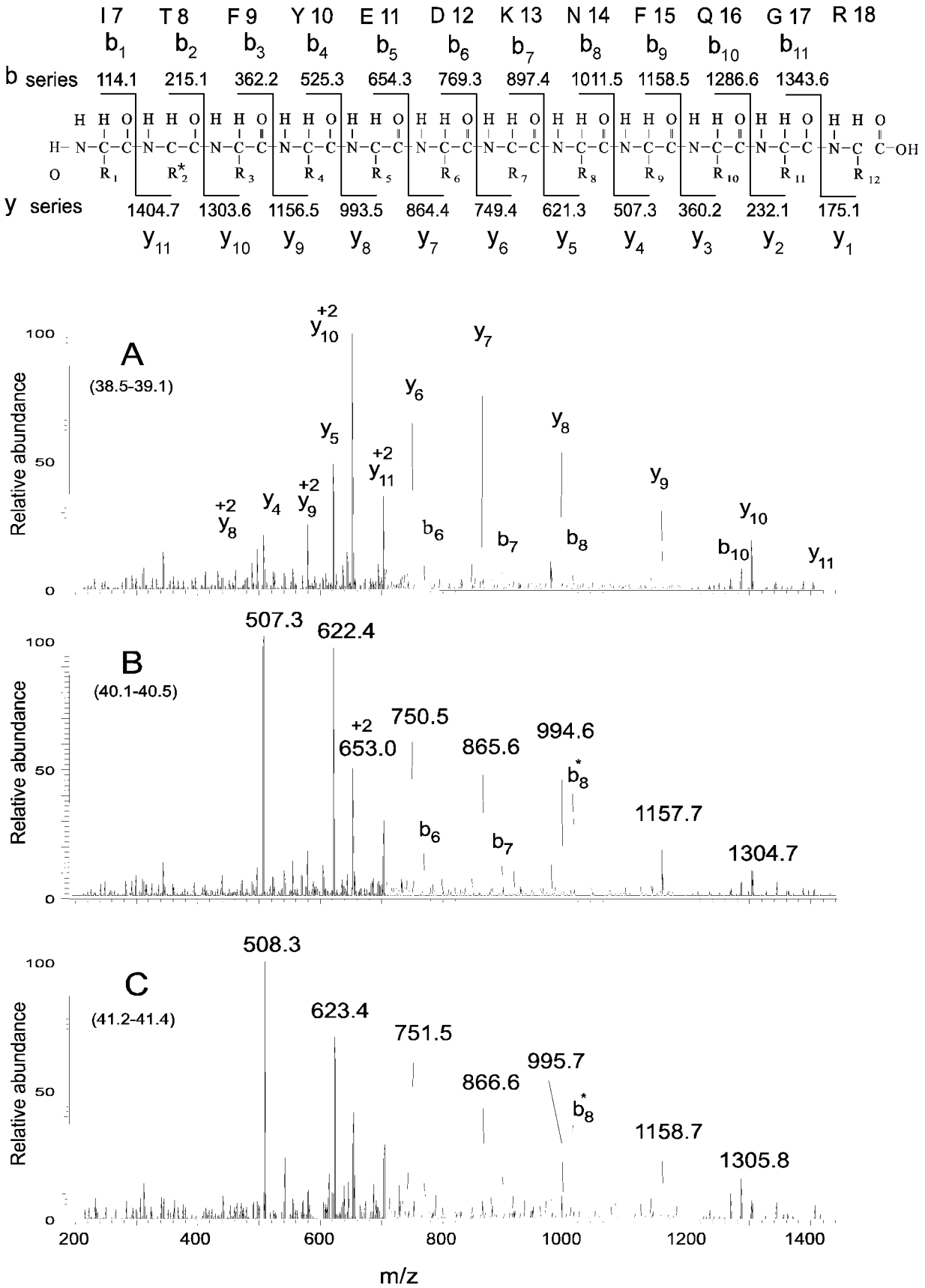

FIGURE 6: MS/MS spectra illustrating deamidation at Asn 14 and Gln 16 of γS-crystallin. The amino acid sequence of peptide 7−18 (T3+T4) and expected y- and b-fragments are given at the top of the figure. (A) the MS/MS spectrum of the unmodified peptide, which eluted at 38.8 min. All y- and b-fragments have the expected masses for the sequence 7−18 of γS. (B) the MS/MS spectrum of the peptide eluting at 40.3 min. The increase in mass for y_5 (622.4), y_6 (750.5), y_7 (865.6), and b_8*-fragments (1012.5) indicate deamidation at Asn 14. (C) The MS/MS spectrum of the peptide eluting in the front part of the peak at 41.6 min. Members of the y series, y_5 (623.4) and larger, show an increase of 2 Da, indicating deamidation at both Asn 14 and Gln 16.

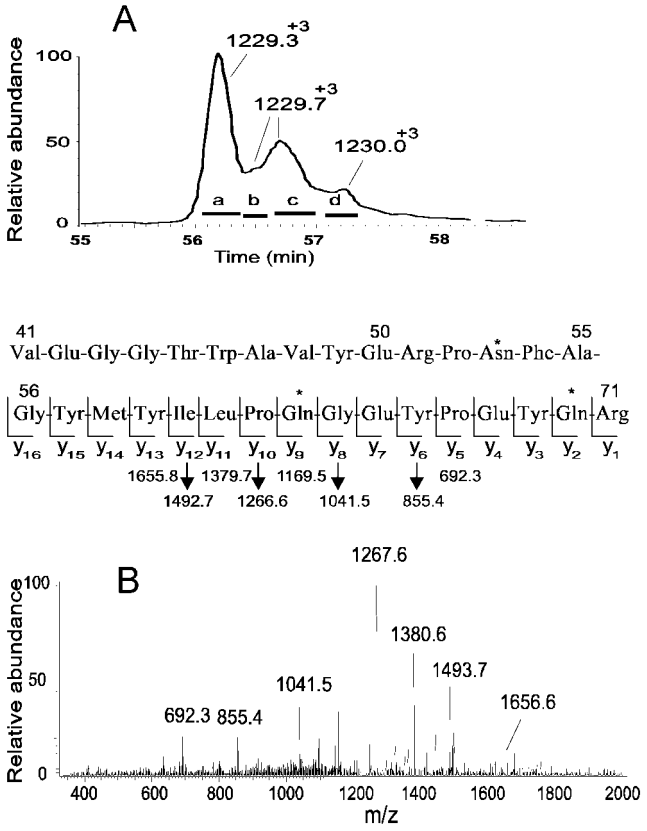

FIGURE 7: An example of using the zoom scan mode and MS/MS analysis for detection of deamidated residues. (A) The total ion current of the reversed phase HPLC of the tryptic digest of γS-crystallins from the water-insoluble high molecular weight proteins of a nuclear cataract monitored in the zoom mode at *m/z* 1229.5 ± 5.0. The masses of the triply charged peptides eluting in each peak are given in the figure. They correspond to peptides with masses of 3685.1, 3686.1, and 3687.1 Da. (B) The MS/MS spectrum of the deamidated peptide eluting in region "b". The sequence of peptide 41−71 and the expected *m/z* values for some fragments of the y-series from the C-terminal region are given at the top. The *m/z* values for y_5, y_6, and y_8 indicate Gln 70 is not deamidated, while increased *m/z* values for y_{10}−y_{13} show deamidation at Gln 63. The asterisks mark potential deamidation sites in peptide 41−71.

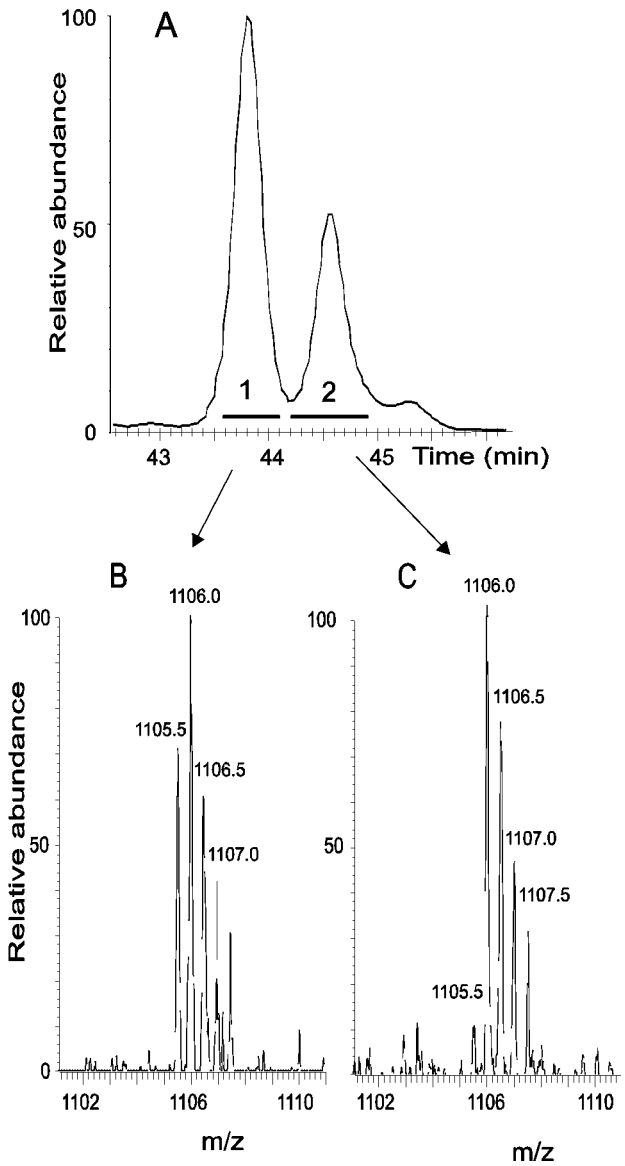

FIGURE 8: Quantification of deamidation at Gln 53. (A) Total ion currents due to peptide 41−59 (MH^+ 2210.0) obtained in the zoom scan mode (*m/z* 1106 ± 5) for an HPLC/MS analysis of a tryptic digest of γS. The identity of the peptide was determined from MS/MS spectra. The small peak eluting at 45.6 min is due to a peptide from γC-crystallin. (B) MS spectrum showing the doubly charged ion of the peptide eluting in peak 1 of panel A. (C) MS spectrum showing the doubly charged ion of the peptide eluting in peak 2 of panel A. The 1 Da increase in the mass of the peptide in peak 2 indicates deamidation at Asn 53.

masses of y_5, y_6, and y_8. The MS/MS fragmentation pattern of the peptide eluting in the "b" region is shown in Figure 7B. From the masses of the y_5, y_6, and y_8 fragments, it was concluded that Gln 70 is not modified. Once the status of Gln 70 was established, the masses at y_{10}−y_{13} gave information about Gln 63. The increase of one mass for these peaks indicated Gln 63 was deamidated. The MS/MS fragments yielding direct information about Asn 53 were weak. However, the status of Asn 53 could be deduced from other information. Since the mass of intact peptide from region "b" indicated only one deamidation and it was already established that Gln 63 was deamidated, Asn 53 was unmodified.

Similar reasoning from MS/MS spectra was used to deduce which residues were modified in peptides eluting in the other regions in Figure 7A. The MS/MS spectrum for the peptides in region "a" supported the conclusion that it was unmodified, giving the expected masses for fragments y_5, y_6, and y_8 as well as y_{10}−y_{13}. In the MS/MS spectrum for region "c", fragments y_5−y_8 and y_{10}−y_{13} indicated no deamidation at either Gln 63 or Gln 70. Because the mass of the intact peptide from region "c" clearly included one deamidation, it could be deduced that the peptide eluting in region "c" was deamidated at Asn 53. Analysis of region "d" indicated deamidation at both Gln 63 and Asn 53.

Confirmation of the deamidations in peptide 41−71 and quantitation of the extent of deamidation at each site were obtained from shorter tryptic peptides (residues 41−59 and 60−71) obtained by digestion at a higher trypsin-protein ratio, which yielded a chymotryptic-like cleavage at Tyr 59. The only potential deamidation site in peptide 41−59 is Asn 53. Analysis of the MS zoom scans (*m/z* 1106 ± 5) for the two species of the peptide as they eluted from HPLC (Figure 8) indicated that Asn is 35% deamidated. Similar analysis of the MS zoom scans for peptide 60−71, which includes Gln 63 and Gln 70, showed about 20% deamidation. The

Table 2: Deamidation Sites in γS-Crystallin Isolated from Nuclear Cataracts

residue(s)	peptide (residues)	analyzed ion (m/z)	method of analysis	extent of deamidation	
				water-soluble	water-insoluble
Asn 14 Gln 16	T3+T4 (7−18)	758.5^{+2}	UV/ICb[a]	Asn 14, 10 ± 3% Gln 16, <5%	Asn 14, 60 ± 10% Gln 16, <20%[e]
Asn 37	T7 * (36−40)	621.5^{+1}	isotopic pattern, MS/MS[b]	15 ± 4%	15 ± 6%
Asn 53	T8 (41−71) (41−59)	1229.5^{+3} 1106.0^{+2}	ICz,[c] MS/MS ICz, MS/MS	<10%	35 ± 6%
Gln 63	T8 (41−71) (60−71)	1229.5^{+3} 747.0^{+2}	ICz, MS/MS SIM[d]	<10%	20 ± 5%
Gln 70	(60−71)	747.0^{+2}	MS/MS	<10%	<10%
Asn 76	T9 (72−78)	891^{+1}	ICz, UV	<5%	8 ± 3%
Gln 92	T11 (84−94)	1156.5^{+1}	UV/IC	<10%	20 ± 6%
Gln 96	T12 (95−100)	777.5^{+1}	isotopic pattern	<5%	<5%
Gln 106 Gln 120	T13 (101−124)	966.0^{+3}	ICz, MS/MS	Gln 106, <10% Gln 120, 45 ± 10%	Gln 106, <10% Gln 120, 60 ± 12%
Asn 143	T15 (131−145)	950.0^{+2}	UV/ICb	20 ± 5%	50 ± 6%
Gln 148	T17+T18 (148−154)	907.5^{+1}	isotopic pattern	<5%	<5%
Gln 170	T20 (158−173)	865.7^{+2}	Isotopic pattern	<5%	<5%

[a] ICb, ion current of the base peak. [b] MS/MS, tandem mass spectrometry. [c] ICz, ion current of zoom scans for specified ions. [d] SIM, selected ion monitoring. [e] Values below the detection limit are indicated by <.

MS/MS spectrum of deamidated peptide 60−71 indicated deamidation only at Gln 63; no deamidation at Gln 70 was detected.

Another peptide that did not elute alone, peptide 101−124 (T13), gave an MS/MS spectrum that did not include a full series of fragments, but there was a sufficient number of strong signals from the y-series to establish the deamidation status of the residues. Selective ion monitoring of peptide 101−124, which contains Gln 106 and Gln 120, showed approximately 60% deamidation. The MS/MS spectrum of deamidated peptide 101−124 showed deamidation at Gln 120, but there was no evidence of deamidation at Gln 106. Neither was deamidation at Gln 106 observed in peptide 101−112 produced by Asp-N digestion of deamidated peptide 101−124.

Minor levels of deamidation were also found at Asn 76 and Gln 92. Because the deamidated forms of peptide 72−88 (T9) and peptide 84−94 (T11) coeluted with other peptides, zoom scans were used to determine the extent of deamidation. Deamidation data are summarized in Table 2.

Several tryptic peptides of γS with potential deamidation sites eluted as single peaks. The isotopic patterns of these tryptic peptides were examined to determine whether there was coelution of deamidated and nondeamidated forms. With the conditions used in this study, deamidation at 10% or more is reliably detected even when the amidated and deamidated peptides elute in a single chromatographic peak. Examination of isotopic patterns gave no evidence for deamidation at Gln 96, Gln 148, and Gln 170 (Table 2).

In analyzing the extent of deamidation at each site in γS, the possibility that deamidated and nondeamidated peptides were cleaved at different rates was also considered. The presence of acidic residues in the vicinity of Lys or Arg residues decreases the rate of the hydrolysis (*32*). For example, at a trypsin/γS-crystallin ratio of 1:50, the predominant tryptic peptide is 7−18 instead of two peptides, 7−13 and 14−18, due to the presence of Asp 12 near the cleavage site at Lys 13. Theoretically, deamidation of Gln 148 might result in resistance of the Arg 147−Glu 148 peptide bond to tryptic cleavage. Therefore, in a tryptic digest one might expect to see peptides 146−147 and 148−153 when residue 148 is Gln, but peptide 146−153 when Gln 148 is deamidated. The digests were examined for this type of behavior, but it was not detected.

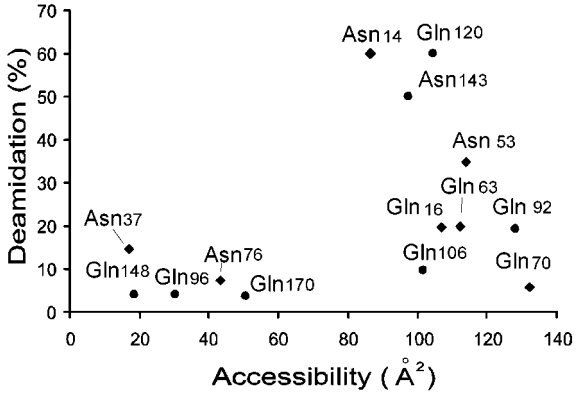

FIGURE 9: Relationship between the surface accessibility and the percent deamidation at glutamines and asparagines in γS-crystallin. Surface accessibilities were calculated (●) from the crystal structure of human γS or (♦) from the homologous residues in bovine γB-crystallins.

Analysis of the extent of deamidation in soluble γS-crystallins isolated from the same nuclear cataracts using similar procedures showed deamidation at the same sites as in the insoluble γS-crystallin, although the level of deamidation was lower, particularly at Asn 14, Asn 35, and Asn 143 (Table 2).

Deamidation and Three Dimensional Structure. The crystal structure of the C-terminal region of human γS-crystallin (*23*) and the homology of the N-terminal regions of human γS and bovine γB, whose crystal structure has been determined (*28*), permitted calculation of the surface accessibility of each of the glutamines and asparagines. Surface accessibility of Asn and Gln residues in human γS-crystallin ranged from 16 to 136. The percent deamidation at each glutamine and asparagine, plotted versus these calculated surface accessibilities (Figure 9), showed minimal deamidation for residues with accessibility numbers less than 80. The extent of deamidation for those with accessibility greater than 80 varied greatly, suggesting that exposure is require for deamidation, but is not the only determining factor. Although two residues with high accessibility, Gln 106 and Gln 70, had minimal deamidation, all sites with

extensive deamidation had high accessibility. Also, all residues with low surface accessibility had little deamidation.

DISCUSSION

Aging and the development of cataract in the lens are associated with accumulation of insoluble HMW proteins, especially in the nucleus. These HMW proteins are formed by disulfide bonds and also by nondisulfide cross-links. A substantial portion of the insoluble HMW protein is intermolecularly disulfide bonded γS-crystallins. Analysis of these γS-crystallins liberated from HMW assemblies by DTT treatment showed the principal modification is deamidation, most extensively at Asn 14, Asn 53, Gln 120, and Asn 143.

Deamidation of lens crystallins was first proposed to explain the increased acidity of lens crystallins associated with aging (*33*, *34*). Later, when phosphorylated crystallins were observed, the increase in acidity was attributed to phosphorylation (*35*, *36*). We now know that deamidation, phosphorylation, and modified lysine residues (*37*−*42*) all contribute to acidification, with deamidation as the most frequent modification of the human crystallins (*7*−*9*, *11*, *12*, *43*, *44*).

Although this is the first report in which deamidation at each glutamine and asparagine residue of γS-crystallin has been quantified, there are previous reports of deamidation at various sites in both water-soluble (*8*) and water-insoluble (*12*) γS-crystallins from clear lenses and in γS-crystallins from cataractous lenses (*15*). There is also a report in which four of the 14 possible deamidation sites in γS-crystallins from the central region of clear old human lenses were examined (*45*). This investigation found no evidence for deamidation at Gln 92, Gln 96, Asn143, and Gln 170. The investigators suggested that γS-crystallin contains some glutamine and asparagine residues that are extremely resistant to in vivo deamidation, consistent with the biological clock hypothesis suggesting that resistance to deamidation is a common property of long-lived proteins (*46*). This hypothesis, which is based on an observation that the in vivo lifetime of some proteins correlates with their total amide content, proposes that proteins with fewer glutamines and asparagines have longer lifetimes because deamidation marks the protein for degradation (*46*). In addition, observation that the nearest neighbor C-terminal to the amide in the primary sequence affects the rate of deamidation of peptides in vitro (*47*, *48*) suggested a possible mechanism for timing of protein deamidation and removal.

Data from lens crystallins are unlikely to be appropriate evidence for the biological clock hypothesis. Lens crystallins have much longer lifetimes than the proteins used to deduce the correlation (*46*). According to that correlation, γS-crystallin, which has 8% glutamines and asparagines, would be expected to have a half-life of about 10 days, but in reality γS is present for the lifetime of the lens. In addition, the nearest neighbors to glutamines and asparagines of γS did not show the same influence on in vivo deamidation of γS-crystallins from cataractous lenses that they exhibited for deamidation of peptides in vitro (*47*, *48*). Rate constants have been determined for deamidation of asparagine containing peptides with various neighbors (*48*). Because similar data are not yet available for glutamine, we used the rate constants determined by Robinson et al. (*48*), assuming the rate of deamidation of glutamines and asparagines might be similarly affected by nearest neighbors, to explore the relationship between these rate constants and the extent of deamidation. We found no correlation ($r = -0.085$, $n = 14$). When rate constants and deamidation were compared for only the nine residues with accessibilities values above 70, the correlation was positive ($r = 0.484$), but with this limited number of residues, it did not attain significance. These data suggest that the influence of the nearest neighbors on deamidation might become evident when residues have adequate surface exposure. A recent publication exploring the relative importance of primary and three-dimensional structure in deamidation of asparagine residues found 60% determined by primary structure and 40% by three-dimensional structure (*27*). Examination of the nearest neighbors of the deamidated residues in our data for γS-crystallins from cataractous lenses indicates that the most notable sequence feature associated with deamidation is the frequency of adjacent prolines and phenylalanines. Since nearby prolines often contribute to increased exposure, it may be that it is the exposure rather than the proline itself that affects deamidation. Perhaps, the longevity of the crystallins is better attributed to a lack of degradation processes in the lens.

In this report, the extent of deamidation was determined for all the asparagines and glutamines of γS-crystallin from nuclear cataracts. Comparison of deamidation in water-soluble and water-insoluble γS-crystallins demonstrated that the water-insoluble crystallins had more deamidation, particularly at Asn 14, Asn 53, and Asn 143. Previous studies indicated that water-insoluble crystallins include more modification (*12*), but this is the first report comparing all the glutamines and asparagines of one crystallin. Increased deamidation of the water-insoluble γS-crystallins also supports the hypothesis that the charge introduced by deamidation contributes to protein unfolding and insolubility. Besides introducing a negative charge at the neutral asparagine, deamidation may be accompanied by racemization and isomerization of aspartic residues (*49*). The formation of β-aspartate, which involves addition of extra carbons to the polypeptide backbone, may destabilize the protein structure (*23*).

On the basis of the crystal structure of the C-terminal domain of γS-crystallin, Purkiss et al. (*23*) have suggested that two glutamines, Gln 106 and Gln 120, are in positions where their deamidation could adversely affect lattice interactions. Deamidation at Gln 106 was below the detection limit, but Gln 120 was 45% deamidated in water-soluble γS and 60% deamidated in water-insoluble γS. The extensive deamidation of Gln 120 even in the water-soluble crystallins suggests that deamidation at this residue has little effect on the protein solubility. The extensive deamidation at Asn 143, both from the water-soluble (20%) and water-insoluble (50%) γS-crystallins, is of particular interest because it has previously been observed in γS-crystallin from senile cataracts, but not age-matched clear lenses (*45*). The deamidations at Asn 14, Asn 143, and Asn 53, which are the most notable differences between the soluble and insoluble γS-crystallins, appear to be the most likely to affect γS-crystallin solubility.

The high levels of deamidation among the γS-crystallin from the HMW portion of the nuclear crystallins permitted comparison of deamidation at glutamines and asparagines with surface accessibility. For the residues in the C-terminal

half, the surface accessibility was determined from the crystal structure for this portion of human γS-crystallin (*23*). The calculated exposures for residues in the N-terminal portion relied on the high homology of human γS and bovine γB (*28*). The relationship between deamidation and surface exposure shows very little deamidation for residues that have an accessibility less than 60−80 Å^2, and a large variation for residues with exposure above the threshold. For example, Gln 106 and Gln 120 have similar accessibilities, but deamidation at Gln 106 is below the detection limit while Gln 120 is 60% deamidated. The crystal structure suggests that this difference may be due to hydrogen bonding of Gln 106 to the carbonyl oxygen of Met 107. Surface exposure appears to be a prerequisite for deamidation, but for those residues that have high accessibility, other factors determine the extent of deamidation.

ACKNOWLEDGMENT

Lenses were obtained through the office of Dr. Kemper Campbell, Lincoln, NE. The authors appreciate helpful discussions with Dr. Christine Slingsby and Dr. David Beebe.

REFERENCES

1. Hoenders, H. J., and Bloemendal, H. (1981) in *Molecular and Cellular Biology of the Eye Lens* (Bloemendal, H., Ed.) pp 279−326, John Wiley and Sons, New York.
2. Kramps, H. A., Hoenders, H. J., and Wollensak, J. (1976) *Biochim. Biophys. Acta 434*, 32−43.
3. Truscott, R. J. W., and Augusteyn, R. C. (1977) *Exp. Eye Res. 24*, 159−170.
4. Bessems, G. J. H., Hoenders, H. J., and Wollensak, J. (1983) *Exp. Eye Res. 37*, 627−637.
5. Kamei, A., Iwata, S., and Horwitz, J. (1987) *Jpn. J. Ophthalmol. 31*, 433−439.
6. Voorter, C. E. M., Roersma, E. S., Bloemendal, H., and de Jong, W. W. (1987) *FEBS Lett. 221*, 249−252.
7. Groenen, P. J. T. A., van Dongen, M. J. P., Voorter, C. E. M., Bloemendal, H., and de Jong, W. W. (1993) *FEBS Lett. 322*, 69−72.
8. Hanson, S. R. A., Smith, D. L., and Smith, J. B. (1998) *Exp. Eye Res. 67*, 301−312.
9. Takemoto, L., and Boyle, D. (1998) *Exp. Eye Res. 67*, 119−120.
10. Takemoto, L., and Boyle, D. (1998) *Biochemistry 37*, 13681−13685.
11. Lund, A. L., Smith, J. B., and Smith, D. L. (1996) *Exp. Eye Res. 63*, 661−672.
12. Hanson, S. R. A., Hasan, A., Smith, D. L., and Smith, J. B. (2000) *Exp. Eye Res. 71*, 195−207.
13. Takemoto, L., Emmons, T., and Granstrom, D. (1990) *Curr. Eye Res. 9*, 793−797.
14. Takemoto, L., and Boyle, D. (1999) *Mol. Vis. 5*, 2−8.
15. Takemoto, L., and Boyle, D. (2000) *Mol. Vis. 6*, 164−168.
16. Harding, J. J., and Crabbe, M. J. C. (1984) in *The Eye* (Davson, H., Ed.) pp 207−492, Academic Press, Orlando, Fl.
17. Spector, A., and Roy, D. (1978) *Proc. Natl. Acad. Sci. U.S.A. 75*, 3244−3248.
18. Takemoto, L. J., and Azari, P. (1977) *Exp. Eye Res. 24*, 63−70.
19. Ortwerth, B. J., and Olesen, P. R. (1992) *Exp. Eye Res. 55*, 777−783.
20. Harding, J. J. (1973) *Exp. Eye Res. 17*, 377−383.
21. Bettelheim, F. A., Siew, E. L., and Chylack, L. T., Jr. (1981) *Invest. Ophthalmol. Vis. Sci. 20*, 348−354.
22. Zarina, S., Zhao, H. R., and Abraham, E. C. (2000) *Mol. Cell Biochem. 210*, 29−34.
23. Purkiss, A. G., Bateman, O. A., Goodfellow, J. M., Lubsen, N. H., and Singsby, C. (2002) *J. Biol. Chem.*, 4199−4205.
24. Pirie, A. (1968) *Invest. Ophthalmol. 7*, 634−650.
25. Laemmli, U. K. (1970) *Nature* (*London*) *277*, 680−685.
26. Courchesna, P. L., and Patterson, S. D. (1999) in *Methods in Molecular Biology* (Link, A. L., Ed.) pp 487−511, Humana Press, Totowa, NJ.
27. Robinson, N. E., and Robinson, A. B. (2001) *Proc. Nat. Acad. Sci. U.S.A. 98*, 4367−4372.
28. Kumaraswamy, V. S., Lindley, P. F., Slingsby, C., and Glover, I. A. (1996) *Acta Crystallogr. D52*, 611−622.
29. Hubbard, S. J., and Thornton, J. M. (1993) NACCESS, computer program, Department of Biochemistry and Molecular Biology, University College, London.
30. Fujii, N., Ishibashi, Y., Satoh, K., Fujino, M., and Harada, K. (1994) *Biochim. Biophys. Acta 1204*, 157−163.
31. Fujii, N., Momose, Y., Ishii, N., Takita, M., Akaboshi, M., and Kodama, M. (1999) *Mech. Ageing Dev. 107*, 347−358.
32. Landon, M., and Piskiewicz, D. (1971) *J. Biol. Chem. 246*, 2374−2399.
33. van Kleef, F. S. M., de Jong, W. W., and Hoenders, H. J. (1975) *Nature* (*London*) *258*, 264−266.
34. van Kleef, F. S. M., Willems-Thijssen, W., and Hoenders, H. J. (1976) *Eur. J. Biochem. 66*, 477−483.
35. Chiesa, R., Gawinowicz-Kolks, M. A., and Spector, A. (1987) *J. Biol. Chem. 262*, 1438−1441.
36. Chiesa, R., Gawinowicz-Kolks, M. A., Kleiman, N. J., and Spector, A. (1988) *Exp. Eye Res. 46*, 199−208.
37. Miesbauer, L. R., Zhou, X., Yang, Z., Yang, Z., Sun, Y., Smith, D. L., and Smith, J. B. (1994) *J. Biol. Chem. 269*, 12494−12502.
38. Lin, P. P., Barry, R. C., Smith, D. L., and Smith, J. B. (1998) *Protein Sci. 7*, 1452−1457.
39. Lin, P., Smith, D. L., and Smith, J. B. (1997) *Exp. Eye Res. 65*, 673−680.
40. Ma, Z., Hanson, S. R., Lampi, K., David, L., Smith, D. L., and Smith, J. B. (1998) *Exp. Eye Res. 67*, 21−30.
41. Lampi, K. J., Ma, Z., Hanson, S. R. A., Azuma, M., Shih, M., Shearer, T. R., Smith, D. L., Smith, J. B., and David, L. L. (1998) *Exp. Eye Res. 67*, 31−43.
42. Lapko, V. N., Smith, D. L., and Smith, J. B. (2001) *Protein Sci. 10*, 1130−1136.
43. Takemoto, L. (1999) *Exp. Eye Res. 68*, 641−645.
44. Zhang, Z., Smith, D. L., and Smith, J. B. (2001) *Eur. J. Mass Spectrom. 7*, 171−179.
45. Takemoto, L., and Boyle, D. (2000) *J. Biol. Chem. 275*, 26109−12.
46. Robinson, A. B., and Rudd, C. J. (1974) *Curr. Top. Cell Regul. 8*, 247−295.
47. Tyler-Cross, R., and Schirch, V. (1991) *J. Biol. Chem. 266*, 22549−22556.
48. Robinson, N. E., and Robinson, A. B. (2000) *Proc. Natl. Acad. Sci. U.S.A. 98*, 944−949.
49. Fujii, N., Matsumoto, S., Hiroki, K., and Takemoto, L. (2001) *Biochim. Biophys. Acta 1549*, 179−187.

BI015924T